

promoting access to White Rose research papers



Universities of Leeds, Sheffield and York
<http://eprints.whiterose.ac.uk/>

This is the author's version of an article published in the **Journal of Biomechanics**

White Rose Research Online URL for this paper:

<http://eprints.whiterose.ac.uk/id/eprint/75940>

Published article:

Meng, Q, Gao, L, Liu, F, Yang, P, Fisher, J and Jin, Z (2010) *Contact mechanics and elastohydrodynamic lubrication in a novel metal-on-metal hip implant with an aspherical bearing surface*. *Journal of Biomechanics*, 43 (5). 849 - 857.

<http://dx.doi.org/10.1016/j.jbiomech.2009.11.018>

Published by Journal of Biomechanics as an Original Article (2010; 43 (5): 849-857)

**Contact mechanics and elastohydrodynamic lubrication in a
novel metal-on-metal hip implant with an aspherical bearing
surface**

Qingen Meng^{a,*}, Leiming Gao^a, Feng Liu^a,
Peiran Yang^b, John Fisher^a, Zhongmin Jin^a

^a Institute of Medical and Biological Engineering,
School of Mechanical Engineering,
University of Leeds, UK

^b School of Mechanical Engineering,
Qingdao Technological University, China

* Corresponding author

Tel: 44 113 343 8893

Fax: 44 113 242 4611

Email: q.meng@leeds.ac.uk

Abstract:

Diameter and diametral clearance of the bearing surfaces of metal-on-metal hip implants and structural supports have been recognized as key factors to reduce the dry contact and hydrodynamic pressure and improve lubrication performance. On the other hand, application of aspherical bearing surfaces can also significantly affect the contact mechanics and lubrication performance by changing the radius of the curvature of a bearing surface and consequently improving the conformity between the head and the cup. In this study, a novel metal-on-metal hip implant employing a specific aspherical bearing surface, Alpharabola, as the acetabular surface was investigated for both contact mechanics and elastohydrodynamic lubrication under steady state conditions. When compared with conventional spherical bearing surfaces, a more uniform pressure distribution and a thicker lubricant film thickness within the loaded conjunction were predicted for this novel Alpharabola hip implant. The effects of the geometric parameters of this novel acetabular surface on the pressure distribution and lubricant thickness were investigated. A significant increase in the predicted lubricant film thickness and a significant decrease in the dry contact and hydrodynamic pressures were found with appropriate combinations of these geometric parameters, compared with the spherical bearing surface.

Keywords: Contact mechanics, Elastohydrodynamic lubrication, Metal-on-metal hip implants, Aspherical bearing surfaces

1. Introduction

One of the major recent developments of hip implants is the resurgence of the old concept of metal-on-metal (MOM) material combinations, due to the modern technology which can produce accurate bearing surfaces with controlled clearance and surface finish. However, the metallic wear particles produced by MOM hip implants are nanometers in size and high in number (Firkins et al., 2001; Catelas et al., 2004; Brown et al., 2007), and their dissolution results in higher levels of cobalt and chromium ions in the serum, urine, and red blood cells of patients with a MOM bearing (Dobbs and Minski, 1980; Jacobs et al., 1996; Savarino et al., 2002; Skipor et al., 2002). The concerns raised by higher ion levels in patients include delayed type hypersensitivity, tissue toxicity, and carcinogenesis (Doorn et al., 1996; Urban et al., 2000; Hallab et al., 2001; Tharani et al., 2001; Chassot et al., 2004). In spite of these concerns, the full and long term biological response to metallic particles is currently unknown. Therefore, it is necessary to minimize wear in MOM hip implants to avoid the risk of these potential adverse reactions.

Current MOM hip implants typically consist of a cobalt chromium (CoCr) spherical femoral head articulating against a hemispherical acetabular cup of a slightly larger diameter usually with the same metallic material. Besides enhancing the wear-resistance of bearing materials by choosing proper carbon content and using other treatments, improving the lubrication in hip implants is an alternative to reduce wear in terms of avoiding the direct contact between the bearing surfaces. Diameter and diametral clearance of hip bearings have been theoretically and experimentally found to be the key parameters of enhancing lubrication and minimizing wear (Medley et al.,

2001; Smith et al., 2001; Dowson et al., 2004; Rieker et al., 2005; Jin, 2006; Liu et al., 2006b). Other factors such as structural supports and the wall thickness of the cup can also affect the contact pressure and lubrication performance in hip implants (Besong et al., 2001; Jagatia and Jin, 2002; Liu et al., 2003; Liu et al., 2004; Liu et al., 2006b).

Reducing clearance is an important design consideration in wear reduction in MOM hip implants. However such an approach is limited by a number of factors, such as the requirement of higher manufacturing accuracy, the potential clamping and equatorial contact, etc. Theoretically, it is only necessary to improve the conformity and reduce the clearance within the main loaded area, while it is advantageous to increase the clearance in the equatorial region. This is consistent with the modified geometries of the worn bearing surfaces in MOM hip implants (Lee et al., 2008; Tuke et al., 2008). Such a variable clearance can be achieved through using aspherical bearing surfaces. Alparabola acetabular cup surface (Fisher, 1995), is one specific example of aspherical bearing geometries.

Deformation of the bearing surfaces of MOM hip implants under load within the contact zone caused by representative contact pressure is typically of micron proportions, while the calculated film thicknesses are only a few tens of nanometers. The ratio of elastic deformation to film thickness is thus of the order of 10^3 (Dowson, 2006). Therefore, elastohydrodynamic lubrication (EHL) has to be considered to obtain pressure distribution and fluid film thickness of MOM hip implants. Moreover, under heavy load and slow speed conditions like those experienced by hip implants, over most of the EHL conjunction, hydrodynamic pressure is determined by unlubricated contact pressure. Therefore, the study of dry contact mechanics is also

important. The purpose of this study was to investigate the dry contact mechanics and EHL in a MOM total hip replacement (THR) employing an Alparabola cup and a spherical head. The effects of the geometric parameters of the Alparabola surface on dry contact pressure, hydrodynamic pressure and film thickness were investigated. The advantages of Alparabola cup over spherical cup were predicted.

2. Model

The Alparabola surface (Fisher, 1995) defined in equation (1) was employed as the internal bearing surface of an acetabular cup:

$$\frac{x^2}{R_2^2/\alpha} + \frac{(y - R_2 + R_2/\alpha)^2}{R_2^2/\alpha^2} + \frac{z^2}{R_2^2/\alpha} = 1, \quad 0 < \alpha < 1 \quad (1)$$

where x , y and z are Cartesian coordinates defined in Figures 1 and 2; R_2 is the desired minimum radius of curvature; α is the parameter to control the variation rate of the radius of the curvature. Since the resultant load experienced by hip implants is in the direction of about 10° medially to the vertical axis (Bergmann et al., 2001), only the vertical component was considered. If the cup was positioned anatomically with an inclination angle of 45° , the surface above the plane $y - z = 0$ was employed, as shown in Figure 1a. However, in order to facilitate the numerical simulations of the contact mechanics and EHL, for most of the cases studied, the portion of the same Alparabola surface defined by equation (1) above the plane $y = 0$ was employed to obtain a horizontally positioned cup, as shown in Figure 1b. The radius of the spherical head, R_1 , was always equal to R_2 to produce a local zero clearance at the contact point.

Both femoral head and acetabular cup were made of CoCr alloy. The cup thickness of 9.5 mm for a typical 28 mm MOM THR was adopted. The bone and the fixation of the cup were represented by an equivalent support layer 2 mm thick with appropriate mechanical properties (Jagatia and Jin, 2001). All the materials in the models were assumed to be homogeneous and linear elastic.

In the EHL model, since a quasi-static analysis can provide a reasonably accurate estimation for lubricating film thickness (Chan et al., 1998), only steady state conditions were considered. Since the major velocity component is in the flexion/extension direction, only the angular velocity around the z axis was considered with a value of 2 rad/s (Jin, 2006; Jagatia and Jin, 2001; Wang et al., 2004). The vertical load was chosen as 3000 N to represent 4 times normal body weight. The lubricant in artificial hip joints is periprosthetic synovial fluid, which behaves as a powerful non-Newtonian fluid under relatively low shear rates. However, under higher shear rates likely to be experienced in the hip joint ($10^5/s$), it is reasonable to assume the periprosthetic synovial fluid as Newtonian, isoviscous and incompressible (Cook et al., 1978; Yao et al., 2003; Jin, 2006; Wang et al., 2008). A realistic viscosity of 0.002 Pa s was adopted (Yao et al., 2003). The important geometric and mechanical parameters involved are listed in Table 1.

The governing equations of the EHL model were established in spherical coordinates, which are defined in Figure 2. The Reynolds equation for the fluid flow between the bearing surfaces was:

$$\sin \theta \frac{\partial}{\partial \theta} \left(h^3 \sin \theta \frac{\partial p}{\partial \theta} \right) + \frac{\partial}{\partial \phi} \left(h^3 \frac{\partial p}{\partial \phi} \right) = 6\eta\omega R_1^2 \sin^2 \theta \frac{\partial h}{\partial \phi} \quad (2)$$

with the following boundary conditions:

$$p(0, \theta) = p(\pi, \theta) = p(\phi, 0) = p(\phi, \pi) = 0$$

$$\partial p / \partial \phi = \partial p / \partial \theta = 0 \quad (3)$$

The film thickness consisted of the undeformed gap and the elastic deformation of bearing surfaces due to the hydrodynamic pressure:

$$h = R_c - R_1 - e_x \sin \theta \cos \phi - e_y \sin \theta \sin \phi + \delta \quad (4)$$

where R_c is the varying radius of the aspherical cup, which was calculated by substituting the following equations

$$x = R_c \cdot \sin \theta \cdot \cos \phi, y = R_c \cdot \sin \theta \cdot \sin \phi, \text{ and } z = R_c \cdot \cos \theta$$

into equation (1), then solving the resultant quadratic equation with R_c as unknowns.

In addition, the external load components were balanced by the integration of the hydrodynamic pressure:

$$f_x = R_1^2 \int_0^\pi \int_0^\pi p \sin^2 \theta \cos \phi d\theta d\phi = 0$$

$$f_y = R_1^2 \int_0^\pi \int_0^\pi p \sin^2 \theta \sin \phi d\theta d\phi = w_y$$

$$f_z = R_1^2 \int_0^\pi \int_0^\pi p \sin \theta \cos \theta d\theta d\phi = 0 \quad (5)$$

3. Method

3.1. Dry Contact mechanics

Three-dimensional finite element (FE) models incorporating the acetabular cup, the femoral head and the equivalent support were created in I-DEAS (version 11.0) and solved using ABAQUS (version 6.7-1). Both models shown in Figures 1a and 1b were simulated. A mesh convergence study was performed to determine the proper

mesh density. Similar dry contact pressure distributions were predicted by 30×30 elements and 60×60 elements on the contact surface. Although the solutions obtained by the mesh density of 30×30 elements could be considered as convergent, the mesh density of 60×60 elements was employed to produce more accurate results, resulting in a total of approximately 57, 000 8-noded linear brick and 6-noded linear triangular prism elements. The element-based contact surfaces were defined as the interface between the cup and head, with the contact surface of the cup being chosen as the slave surface. The type of the contact pair was defined as “surface to surface”. “Finite sliding” was used as the tracking approach. The option of ‘adjust = 0.0’ was also adopted to avoid the initial overclosure. No friction was considered between the bearing surfaces since its effect in a well lubricated MOM bearing on the contact pressure prediction of hip implant is negligible (Liu et al., 2003).

3.2. Elastohydrodynamic lubrication

The Reynolds equation was solved by a multi-grid (MG) method, while the elastic deformation was calculated using a multi-level multi-integration (MLMI) technique (Gao et al., 2007; Venner, 1991). Three levels of grid were used in the multilevel solver. On the finest level, 257 nodes were arranged in both the θ and ϕ directions (Liu et al., 2006a; Wang and Jin, 2007). The convergence criteria for hydrodynamic pressure and the loads in the y and x directions were kept to be 10^{-4} , 10^{-4} and 10^{-5} respectively.

The elastic deformation coefficients of an Alphasphere cup were approximated by those of a corresponding spherical cup with a radius given by the minimum radius of

the Alphasphere cup. The deformation coefficients of the approximate spherical cup were obtained using the method developed by Wang and Jin (2004). The errors in this approximation were estimated by applying a parabolic pressure distribution (Wang and Jin, 2004) to an Alphasphere cup, then calculating the deformation using both the approximate deformation coefficients and the direct FE method.

4. Results

Figure 3 compares the dry contact pressure distributions obtained from the models with anatomically and horizontally positioned cups. Results shown in Figures 4–12 were obtained from the horizontal cup model. Figure 4 shows the contour plots of dry contact pressure distribution at the bearing surface for different α values with the same R_2 . Figure 5 compares the effect of α on the dry contact pressure along the central line through the contact centre. The effect of different bearing radii (R_2) on dry contact pressure is shown in Figure 6 with a fixed α . The corresponding dry contact pressure along the central line through the contact centre is illustrated in Figure 7.

Figure 8 compares the deformations of an Alphasphere cup ($R_2 = 14$ mm) calculated using the approximate deformation coefficients and the FE method. The contour plots of hydrodynamic pressure for different values of α with the same R_2 are shown in Figure 9. Figure 10 shows the effect of α on the hydrodynamic pressure and film thickness along the central line through the contact centre. In addition, the hydrodynamic pressure and film thickness of a typical 14 mm radius spherical hip implant with a clearance of 30 μm are also plotted in Figure 10. Figure 11 plots the

contours of hydrodynamic pressure for different R_2 with a fixed α . Figure 12 shows the effects of R_2 on the hydrodynamic pressure and film thickness along the central line through the contact centre with a fixed α .

5. Discussion

It is reasonable to use the horizontal cup model shown in Figure 1b to investigate the dry contact mechanics and EHL of the MOM hip implants employing Alpharabola cup. Within the contact area, the same portion of the Alpharabola surface defined in equation (1) was employed by the horizontal cup and the anatomical cup models. Therefore, as expected, the two models produced similar dry contact pressure distributions, with the maximum values of 28.6 MPa and 28.4 MPa respectively, except the contact location was different, as shown in Figure 3. Furthermore, it was shown that a cup inclination angle of up to 45 deg had a negligible effect on the lubricant film thickness and hydrodynamic pressure (Wang and Jin, 2005).

The deformation coefficients of the spherical cup can provide reasonably accurate estimation for the Alpharabola cup. As shown in Figure 8, when $\alpha = 0.9$ ($R_2 = 14$ mm), which represented the largest deviation from a sphere in this study, the maximum difference between deformations calculated using the deformation coefficients of the approximation spherical cup and the FE method was only about 4.5%.

It is interesting to note that the overall dry contact pressure distribution in this novel MOM hip implant is markedly different from that in conventional spherical MOM hip implants (Jagatia and Jin, 2001). Due to an enlarged contact area caused by the reduced effective radial clearance near the contact centre, the maximum dry contact pressure occurred towards the edge of the contact area, rather than at the contact centre, as shown in Figures 4–7. Moreover, since hydrodynamic pressure is largely determined by unlubricated contact pressure, for the same geometric and mechanical parameters, the corresponding profiles and the magnitudes of the hydrodynamic pressures shown in Figures 9–12 closely resembled those of the dry contact pressures shown in Figures 4–7. For example, for the case of $\alpha = 0.99$ and $R_2 = 14$ mm, the maximum and central dry contact pressures were 28.3 MPa and 18.4 MPa, while the corresponding values for hydrodynamic pressure were 27.2 MPa and 18.6 MPa.

A similar pressure distribution was also predicted by Besong et al. (2001) and Jagatia and Jin (2002) for the Ultima prosthesis and Liu et al. (2003; 2004) for the Metasul prosthesis. In Ultima prosthesis, the lower contact pressure at the contact centre was caused by the gap between the acetabular insert and the titanium shell, which allowed the bearing surfaces to be more compliant under loading, leading to increased conformity between femoral head and acetabular cup. In Metasul prosthesis, similar pressure distribution was caused by the UHMWPE backing which also enlarged the contact area. Therefore, it can be expected that the increase in the contact area between bearing surfaces leads to a lower contact pressure at the contact centre. Conformity may be enhanced by both introducing new structure designs, such as Ultima and Metasul prostheses, and employing aspherical bearing surface, such as Alpharabola.

The main parameter governing the conformity between the two bearing surfaces is α which controls the variation in the radius. For a fixed R_2 , a larger α produces a larger conformal area. As shown in Figure 4, an increase in α from 0.9 to 0.99 resulted in a twofold increase in contact area. Dry contact and hydrodynamic pressures are generally determined by load and contact area. For the same load, the larger the contact area, the lower the dry contact and hydrodynamic pressures. As shown in Figures 4 and 9, an increase in α from 0.9 to 0.99 resulted in a decrease in the maximum dry contact and hydrodynamic pressures from 68.9 MPa to 28.4 MPa and from 66.4 MPa to 27.2 MPa, respectively. The desired minimum radius of the cup, R_2 , is another important parameter of the Alpherabola surface which controls the bearing size. An increase in R_2 also results in an increase in contact area. As shown in Figure 6, an increase in R_2 from 14 mm to 20 mm resulted in an increase in the contact area from 74.6 mm² to 109.50 mm². Consequently, dry contact and hydrodynamic pressures in the prosthesis with a larger radius were lower than those of that with a smaller radius, as shown in Figures 6 and 11. The maximum dry contact and hydrodynamic pressures for $R_2 = 14$ mm were 51.9 MPa and 50.5 MPa while 34.21 MPa and 34.3 MPa for $R_2 = 20$ mm.

Since the hydrodynamic pressure at the contact area is largely determined by the unlubricated and frictionless contact pressure, the effect of Poiseuille flow can be neglected and Couette flow dominates. Therefore, a constant film thickness is necessary to keep the flow continuous. Due to the undeformed gap between the cup and the head being more uniform, the film profile in this novel implant was flatter within the contact area than that in the spherical implant, as shown in Figure 10b. It is

also expected that the nearly parallel undeformed gap is helpful for the squeeze-film lubrication action under real walking conditions. Moreover, an increase in either α or R_2 leads to an increase in film thickness due to the increase in the contact area and the reduction in the pressure. As shown in Figures 10b and 12b, the minimum film thickness increased from 0.003 μm to 0.0677 μm when α increased from 0.9 to 0.99, and from 0.008 μm to 0.017 μm when R_2 increased from 14 mm to 20 mm.

The radial clearance at the equatorial region was employed as a reference to compare the pressure and film thickness of this novel hip implant with those of conventional spherical hip implants. The corresponding α to produce an equatorial radial clearance of 30 μm as used in a 14 mm radius spherical bearing is 0.9957. As shown in Figure 10, the Alpharabola cup improved the minimum film thickness by approximately 70%, compared with the spherical one. Such an improvement in film thickness may prevent the bearing surfaces from direct contact and consequently avoid wear. However, it should be recognised that the Alpharabola cup has a larger contact area, and this could potentially increase wear if the lubricant film breaks down. Although the local clearance at the pole of the Alpharabola hip implant is zero, a large equatorial clearance of $(2 - \alpha)^{1/2}R_2 - R_2$ can be formed for the horizontally positioned cup by the continuous and monotonous variation in the radius of the Alpharabola surface. Such a large equatorial clearance is advantageous to avoid the potential clamping and equatorial contact under loading (Farrar and Schmidt, 1997) and when implanted through press-fit (Jin et al., 2006; Yew et al., 2006).

However, the manufacturing of the Alpharabola cup can be potentially more challenging due to the local nonspherical surface. Moreover, the reference zero

clearance of the aspherical cup should be aligned in the direction of the resultant load to obtain an 'optimum' contact position, however, the direction of the resultant load varies during normal walking (Bergmann et al., 2001). Different activities of daily living, such as sitting down and climbing stairs, also have different trajectories of resultant load (Bergmann et al., 2001). Therefore, the ideal 'optimum' contact position is not practical. However, the position of the zero clearance can be chosen according to the direction of either the maximum or the average resultant load of a normal walking gait. Furthermore, both the manufacturing errors and the angles of inclination and anteversion produced during the implantation operation may affect the contact position. Therefore, the sensitivity of the lubrication performance of the Alparabola cup to the manufacturing errors and inclination and anteversion angles of the cup needs to be investigated in the future. Moreover, although it was predicted that the nearly parallel gap between the cup and the head is helpful for the squeeze-film lubrication action, detailed numerical analysis should also be performed to investigate the effect of three-dimensional load and motion, especially under adverse lubrication conditions such as a sudden increase in load or without entraining velocity, associated with start-up and stopping.

6. Conclusion

Both three-dimensional FE dry contact and EHL models were developed for a novel hip implant employing an Alparabola cup and a spherical head. Typical dry contact and hydrodynamic pressure distributions and film profiles were predicted. The effects of the geometric parameters α and R_2 on pressure distribution and fluid film thickness were analyzed. The lubrication performance of this Alparabola hip implant was

compared to that of the spherical hip implant. The following conclusions can be drawn for this novel implant:

- (1) Both the maximum dry contact and hydrodynamic pressures occurred towards the edge of the contact area and consequently an annular maximum pressure distribution was found. Moreover, the film profile was flatter than that in the hip implant with spherical bearing surfaces.
- (2) The increase in either the variation rate of radius (α) or the size (R_2) of the Alparabola surface may enlarge the contact area, reduce the dry contact and the hydrodynamic pressures and consequently improve the film thickness.
- (3) With the same equatorial radial clearance, the pressure of the Alparabola hip implant was much lower and the lubricant film thickness much thicker, compared with the spherical hip implant.

7. Acknowledgement

This work was supported by the Overseas Research Students Award Scheme (ORSAS) to Qingen Meng, and the National Natural Science Foundation of China through grants 50628505 and 50575108.

Conflict of interest statement

There is no conflict of interest involved in publishing this paper except the following:

1. John Fisher is the inventor of the studied Alparabola surface.
2. This work was supported by the ORSAS to Qingen Meng, and the National Natural Science Foundation of China through grants 50628505 and 50575108.

References:

Bergmann, G., Deuretzbacher, G., Heller, M., Graichen, F., Rohlmann, A., Strauss, J., Duda, G. N., 2001. Hip contact forces and gait patterns from routine activities. *Journal of Biomechanics* 34, 859–871.

Besong, A. A., Lee, R., Farrar, R., Jin, Z. M., 2001. Contact mechanics of a novel metal-on-metal total hip replacement. *Proceedings of the Institution of Mechanical Engineers, Part H: Journal of Engineering in Medicine* 215, 543–548

Brown, C., Williams, S., Tipper, J. L., Fisher, J., Ingham, E., 2007. Characterisation of wear particles produced by metal on metal and ceramic on metal hip prostheses under standard and microseparation simulation. *Journal of Materials Science: Materials in Medicine* 18, 819–827.

Catelas, I., Medley, J. B., Campbell, P. A., Huk, O. L., Bobyn, J. D., 2004. Comparison of *in vitro* with *in vivo* characteristics of wear particles from metal-metal hip implants. *Journal of Biomedical Materials Research Part B: Applied Biomaterials* 70B, 167–178.

Chan, F.W., Medley, J.B., Bobyn, J.D., Krygier, J.J., 1998. Numerical analysis of time-varying fluid film thickness in metal-metal hip implants in simulator tests. In: Jacobs, J.J., Craig, T.L. (Eds.), *Alternative Bearing Surfaces in Total Hip Joint Replacement*. Transactions of American Society of Mechanical Engineers STP 1346. ASTM, West Conshohocken, PA, USA, pp. 111–125.

Chassot, E., Irigaray, J. L., Terver, S., Vanneuville, G., 2004. Contamination by metallic elements released from joint prostheses. *Medical Engineering & Physics* 26, 193–199.

Cooke, A. V., Dowson, D., Wright, V., 1978. The rheology of synovial fluid and some potential synthetic lubricants for degenerate synovial joints. *Engineering in Medicine* 7, 66–72.

Dobbs, H. S., Minski, M. J., 1980. Metal-ion release after total hip-replacement. *Biomaterials* 1, 193–198.

Doorn, P. F., Mirra, J. M., Campbell, P. A., Amstutz, H. C., 1996. Tissue reaction to metal on metal total hip prostheses. *Clinical Orthopaedics and Related Research* 329, S187–S205.

Dowson, D., Hardaker, C., Flett, M., Isaac, G. H., 2004. A hip joint simulator study of the performance of metal-on-metal joints. Part II: design. *Journal of Arthroplasty* 19, S124–S130.

Dowson, D., 2006. Tribological principles in metal-on-metal hip joint design. *Proceedings of the Institution of Mechanical Engineers, Part H: Journal of Engineering in Medicine* 220, 161–171.

Farrar, R., Schmidt, M. B., 1997. The effect of diametral clearance on wear between head and cup for metal on metal articulations. 43rd Annual Meeting of the Orthopaedic Research Society, No. 71.

Firkins, P. J., Tipper, J. L., Saadatzadeh, M. R., Ingham, E., Stone, M. H., Farrar, R., Fisher, J., 2001. Quantitative analysis of wear and wear debris from metal-on-metal hip prostheses tested in a physiological hip joint simulator. *Bio-Medical Materials and Engineering* 11, 143–157.

Fisher, J., issued 8 September 1995. Acetabular cup. World Intellectual Property Organization patent, No. WO 95/23566.

Gao, L. M., Meng, Q. E., Wang, F. C., Yang, P. R., Jin, Z. M., 2007. Comparison of numerical methods for elastohydrodynamic lubrication analysis of metal-on-metal hip implants: multi-grid verses Newton–Raphson. *Proceedings of the Institution of Mechanical Engineers, Part J: Journal of Engineering Tribology* 221, 133–140

Hallab, N., Merritt, K., Jacobs, J. J., 2001. Metal sensitivity in patients with orthopaedic implants. *The Journal of Bone and Joint Surgery, American Volume* 83, 428–436.

Jacobs, J. J., Skipor, A. K., Doorn, P. F., Campbell, P., Schmalzried, T. P., Black, J., Amstutz, H. C., 1996. Cobalt and chromium concentrations in patients with metal on metal total hip replacements. *Clinical Orthopaedics and Related Research* 329, S256–S263.

Jagatia, M., Jin, Z. M., 2001. Elastohydrodynamic lubrication of metal-on-metal hip prosthesis under steady-state entraining motion. *Proceedings of the Institution of Mechanical Engineers, Part H: Journal of Engineering in Medicine* 215, 531–541.

Jagatia, M., Jin, Z. M., 2002. Analysis of elastohydrodynamic lubrication in a novel metal-on-metal hip joint replacement. *Proceedings of the Institution of Mechanical Engineers, Part H: Journal of Engineering in Medicine* 216, 185–193.

Jin, Z. M., 2006. Theoretical studies of elastohydrodynamic lubrication of artificial hip joints. *Proceedings of the Institution of Mechanical Engineers, Part J: Journal of Engineering Tribology* 220, 719–727.

Jin, Z. M., Meakins, S., Morlock, M. M., Parsons, P., Hardaker, C., Flett, M., Isaac, G., 2006. Deformation of press-fitted metallic resurfacing cups. Part 1: experimental simulation. *Proceedings of the Institution of Mechanical Engineers, Part H: Journal of Engineering in Medicine* 220, 299–309.

Lee, R., Essner, A., Wang, A., 2008. Tribological considerations in primary and revision metal-on-metal arthroplasty. *The Journal of Bone and Joint Surgery, American Volume* 90 Suppl 3, 118–124.

Liu, F., Jin, Z. M., Grigoris, P., Hirt, F., Rieker, C., 2003. Contact mechanics of metal-on-metal hip implants employing a metallic cup with a UHMWPE backing.

Proceedings of the Institution of Mechanical Engineers, Part H: Journal of Engineering in Medicine 217, 207-213.

Liu, F., Jin, Z. M., Hirt, F., Rieker, C., Roberts P., 2006. Transient elastohydrodynamic lubrication analysis of metal-on-metal hip implant under simulated walking conditions. Journal of Biomechanics 39, 905–914.

Liu, F., Jin, Z. M., Roberts P., Grigoris, P., 2006. Importance of head diameter, clearance, and cup wall thickness in elastohydrodynamic lubrication analysis of metal-on-metal hip resurfacing prostheses. Proceedings of the Institution of Mechanical Engineers, Part H: Journal of Engineering in Medicine 220, 695–704.

Liu, F., Wang, F. C., Jin, Z. M., Hirt, F., Rieker, C., Grigoris, P., 2004. Steady-state elastohydrodynamic lubrication analysis of a metal-on-metal hip implant employing a metallic cup with an ultra-high molecular weight polyethylene backing. Proceedings of the Institution of Mechanical Engineers, Part H: Journal of Engineering in Medicine 218, 261–270.

Medley, J. B., Bobyn, J. D., Krygier, J. J., Chan, F. W., Tanzer, M., Roter, G. E., 2001. Elastohydrodynamic lubrication and wear of metal-on-metal hip implants. In: Claude Rieker, et al. (Eds.), World Tribology Forum in Arthroplasty. Hans Huver, pp. 125–136.

Rieker, C. B., Schon, R., Konrad, R., Liebenritt, G., Gnepf, P., Shen, M., Roberts, P., Grigoris, P., 2005. Influence of the clearance on *in vitro* tribology of large diameter

metal-on-metal articulations pertaining to resurfacing hip implants. *Orthopedic Clinics of North America* 36, 135–142.

Skipor, A. K., Campbell, P. A., Patterson, L. M., Amstutz, H. C., Schmalzried, T. P., Jacobs, J. J., 2002. Serum and urine metal levels in patients with metal-on-metal surface arthroplasty. *Journal of Materials Science: Materials in Medicine* 13, 1227–1234.

Savarino, L., Granchi, D., Ciapetti, G., Cenni, E., Pantoli, A. N., Rotini, R., Veronesi, C. A., Baldini, N., Giunti, A., 2002. Ion release in patients with metal-on-metal hip bearings in total joint replacement: A comparison with metal-on-polyethylene bearings. *Journal of Biomedical Material Research* 63, 467–474.

Smith, S. L., Dowson, D., Goldsmith, A. A. J., 2001. The lubrication of metal-on-metal total hip joints: a slide down the Stribeck curve. *Proceedings of the Institution of Mechanical Engineers, Part H: Journal of Engineering in Medicine* 215, 483–493.

Tharani, R., Dorey, F. J., Schmalzried, T. P., 2001. The risk of cancer following total hip or knee arthroplasty. *The Journal of Bone and Joint Surgery, American Volume* 83, 774–780.

Tuke, M. A., Scott, G., Roques, A., Hu, X. Q., Taylor, A., 2008. Design considerations and life prediction of metal-on-metal bearings: the effect of clearance. *The Journal of Bone and Joint Surgery, American Volume* 90 Suppl 3, 134–141.

Urban, R. M., Jacobs, J. J., Tomlinson, M. J., Gavrilovic, J., Black, J., Peoc'h, M., 2000. Dissemination of wear particles to the liver, spleen, and abdominal lymph nodes of patients with hip or knee replacement. *The Journal of Bone and Joint Surgery, American Volume* 82, 457–477.

Venner, C. H., 1991. Multigrid solution of the EHL line and point contact problems. PhD thesis, University of Twente, Enschede.

Wang, F. C., Jin, Z. M., 2004. Prediction of elastic deformation of acetabular cup and femoral head for lubrication analysis of artificial hip joints. *Proceedings of the Institution of Mechanical Engineers, Part J: Journal of Engineering Tribology* 218, 201–209.

Wang, F. C., Jin, Z. M., 2005. Elastohydrodynamic lubrication modeling of artificial hip joints under steady-state conditions. *Transaction of the ASME, Journal of Tribology* 127, 729–739.

Wang, F. C., Jin, Z. M., 2007. Effect of non-spherical bearing geometry on transient elastohydrodynamic lubrication in metal-on-metal hip joint implants. *Proceedings of the Institution of Mechanical Engineers, Part J: Journal of Engineering Tribology* 221, 379–389.

Wang, F. C., Liu, F., Jin, Z. M., 2004. A general elastohydrodynamic lubrication analysis of artificial hip joints employing a compliant layered socket under steady

state rotation. Proceedings of the Institution of Mechanical Engineers, Part H: Journal of Engineering in Medicine 218, 283–291.

Wang, W. Z., Jin, Z. M., Dowson, D., Hu, Y. Z., 2008. A study of the effect of model geometry and lubricant rheology upon the elastohydrodynamic lubrication performance of metal-on-metal hip joints. Proceedings of the Institution of Mechanical Engineers, Part J: Journal of Engineering Tribology 222, 493–501.

Yao, J. Q., Laurent, M. P., Johnson, T. S., Blanchard, C. R., Crowinshield, R. D., 2003. The influence of lubricant and material on polymer/CoCr sliding friction. Wear 255, 780–784.

Yew, A., Jin, Z. M., Donn, A., Morlock, M. M., Isaac, G., 2006. Deformation of press-fitted metallic resurfacing cups. Part 2: finite element simulation. Proceedings of the Institution of Mechanical Engineers, Part H: Journal of Engineering in Medicine 220, 311–319.

Nomenclature:

$e_x, e_y,$	eccentricity components of the femoral head in x and y directions
f_x, f_y, f_z	calculated load components defined in equation (5)
h	film thickness
p	pressure
R_1	femoral head radius
R_2	desired minimum radius of curvature of the Alparabola surface
R_c	Variable radius of the Alparabola cup
w	applied load in y direction
x, y, z	Cartesian coordinates
α	the parameter to control variation rate of the radius of Alparabola
β	the inclination angle of the cup, 45° in this study
δ	elastic deformation the femoral head and acetabular cup
η	viscosity of synovial fluid
ϕ, θ	angular coordinates in the entraining and side-leakage directions respectively, defined in Figure 2.
ω	angular velocity

Captions

Table 1	Typical input parameters for contact mechanics and EHL analysis
Figure 1	A simple configuration for the MOM hip implant with Alphasphere as the cup bearing surface
Figure 2	Definition of spherical coordinates and spherical mesh grid
Figure 3	Contour of contact pressure (MPa) at the bearing surface of an aspherical hip implant with an Alphasphere cup with different α : (a) 0.9 , (b) 0.95, (c) 0.97, (d) 0.99 ($R_1 = R_2 = 14$ mm)
Figure 4	Comparison of the contact pressure distribution along the central line through the contact centre with different α ($R_1 = R_2 = 14$ mm)
Figure 5	Contour of contact pressure (MPa) at the bearing surface of an aspherical hip implant with an Alphasphere cup with different R_2 : (a) 14 mm , (b) 16 mm, (c) 20 mm ($\alpha = 0.95$ mm)
Figure 6	Comparison of the contact pressure distribution along the central line through the contact centre with different R_2 ($\alpha = 0.95$)
Figure 7	Comparison of the deformation of the aspherical cups calculated by FE model and that calculated by the approximate coefficients under the same pressure distribution
Figure 8	Contour plots of hydrodynamic pressure (MPa) in the aspherical hip implant with an Alphasphere cup for different α : (a) 0.9 , (b) 0.95, (c) 0.97, (d) 0.99 ($R_2 = 14$ mm)
Figure 9	Comparison of (a) pressure distribution and (b) film thickness on the central line along the entraining direction for different α ($R_2 = 14$ mm)
Figure 10	Contour plots of hydrodynamic pressure (MPa) in the aspherical hip implant with an Alphasphere cup for different R_2 : (a) 14 mm, (b) 16 mm, (c) 20 mm ($\alpha = 0.95$)

Figure 11 Comparison of (a) pressure distribution and (b) film thickness on the central line along the entraining direction for different R_2 ($\alpha = 0.95$)

Table 1

Thickness of equivalent support	2 mm
Radius of cup inside surface, R_2	14 - 20 mm
Radius of head, R_1	14 - 20 mm
Cup wall thickness	9.5 mm
Elastic modulus of the metal	210 GPa
Elastic modulus of equivalent support	2.27 GPa
Poisson's ratio of metal	0.3
Poisson's ratio of equivalent support	0.23
Load	3000 N
Viscosity of synovial fluid	0.002 Pas
Angular velocity	2 rad/s

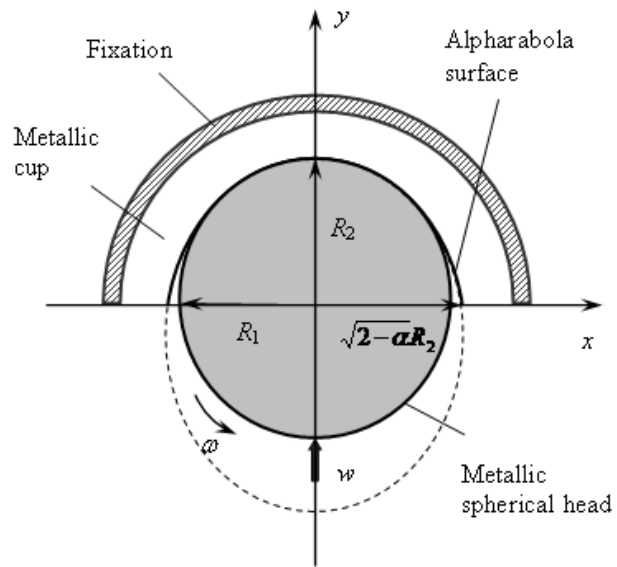


Figure 1

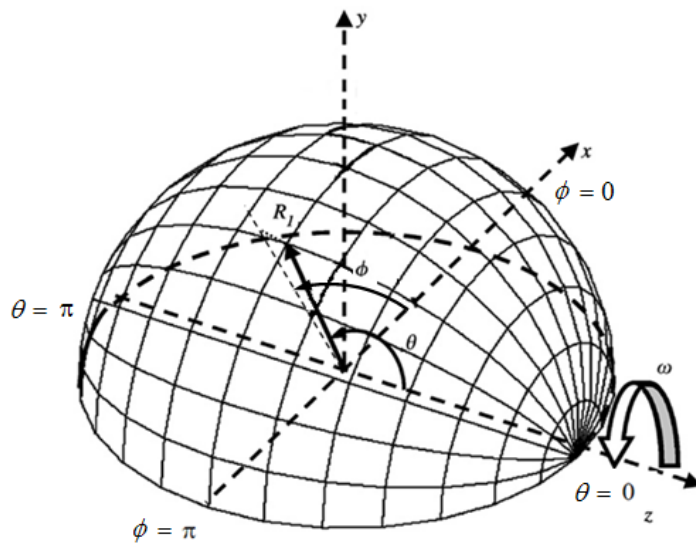


Figure 2

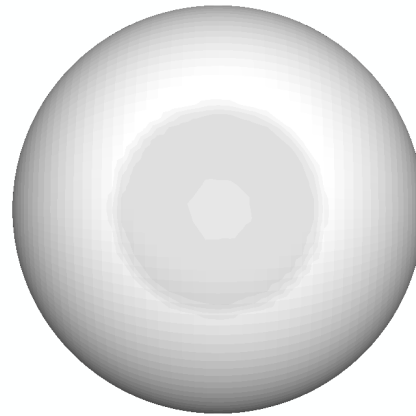
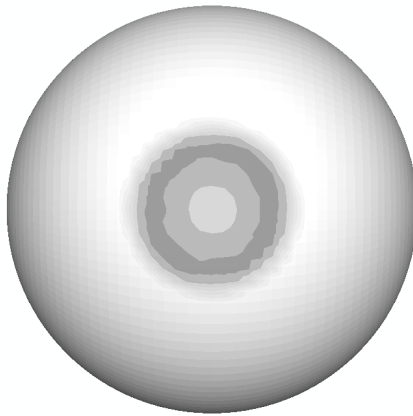
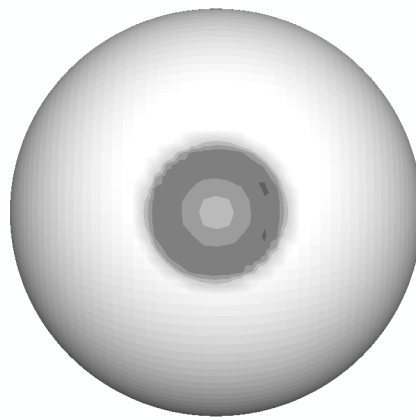
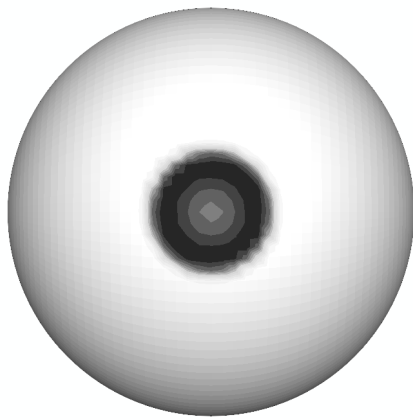
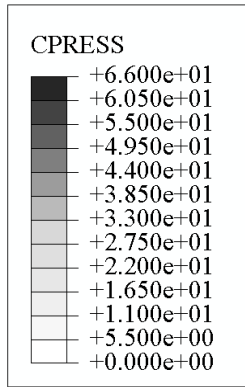


Figure 3

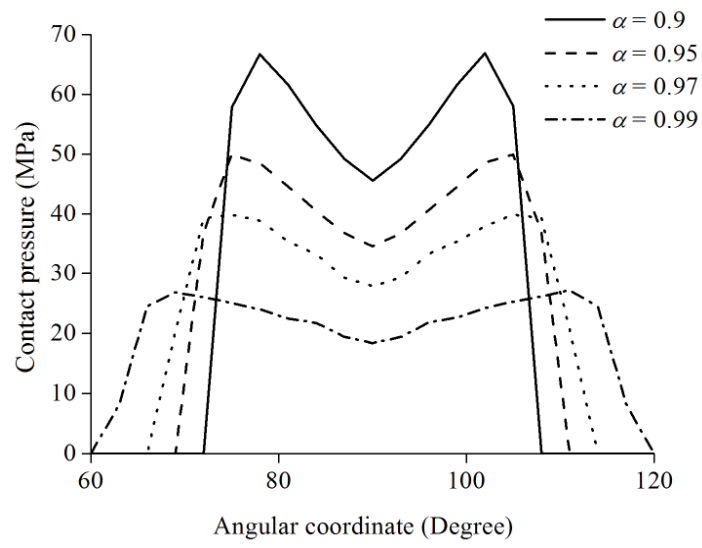
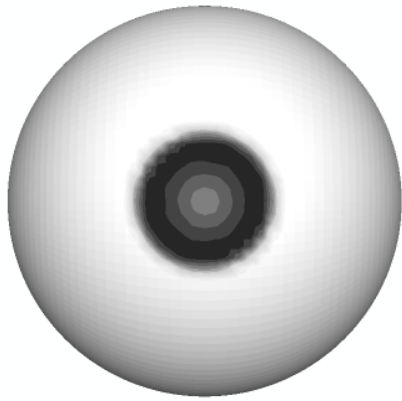
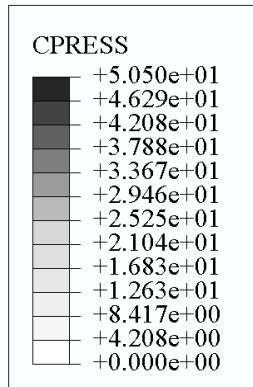
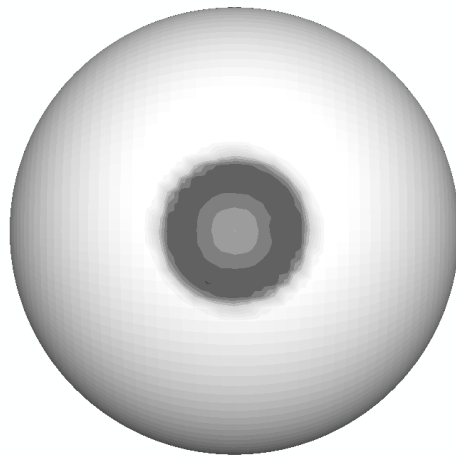


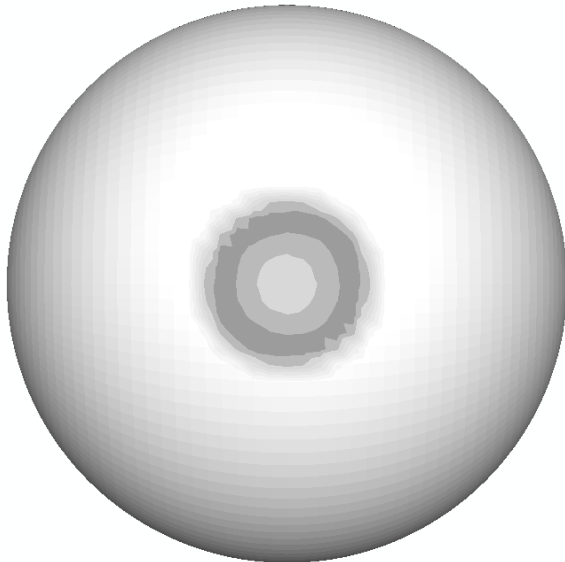
Figure 4



(a)



(b)



(c)

Figure 5

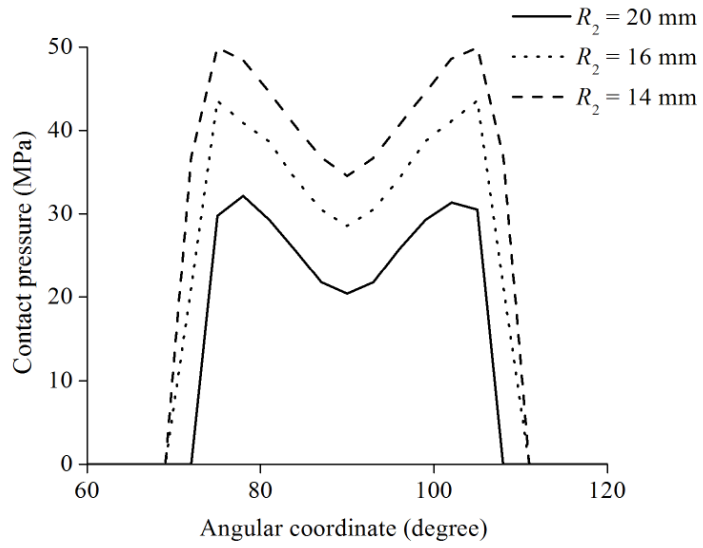


Figure 6

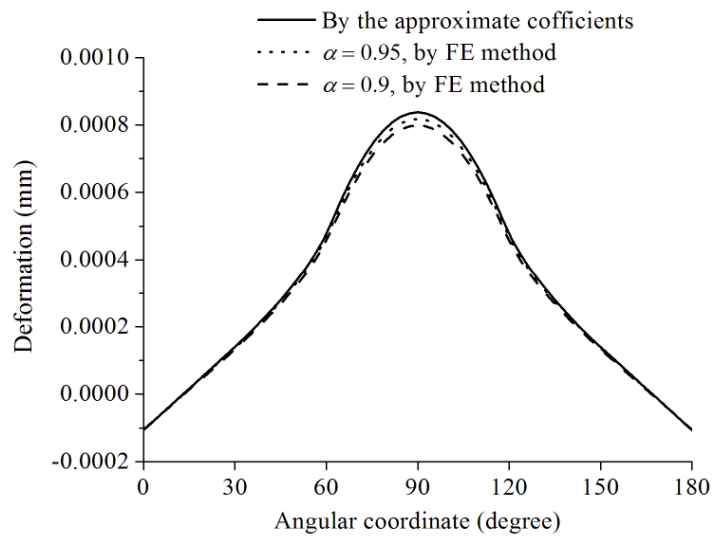


Figure 7

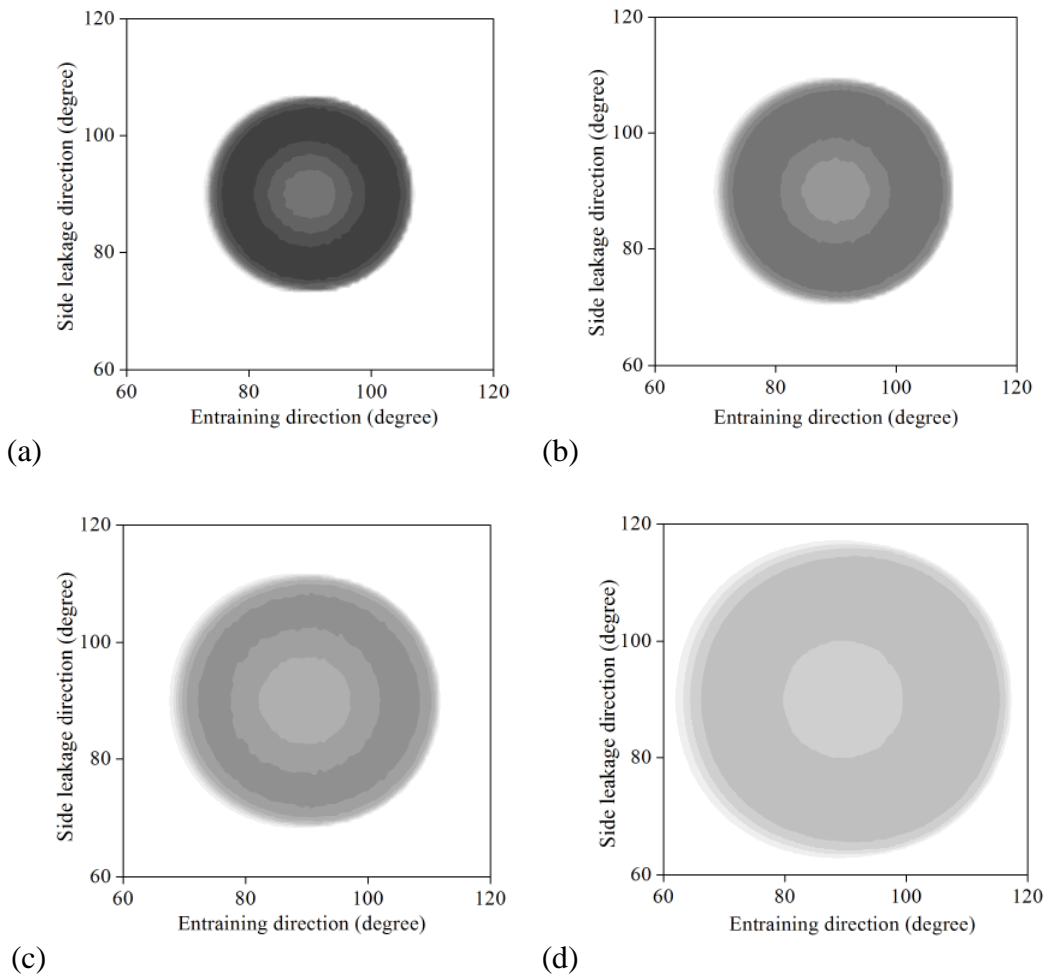
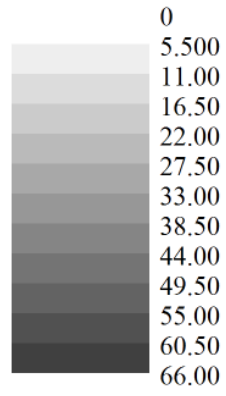
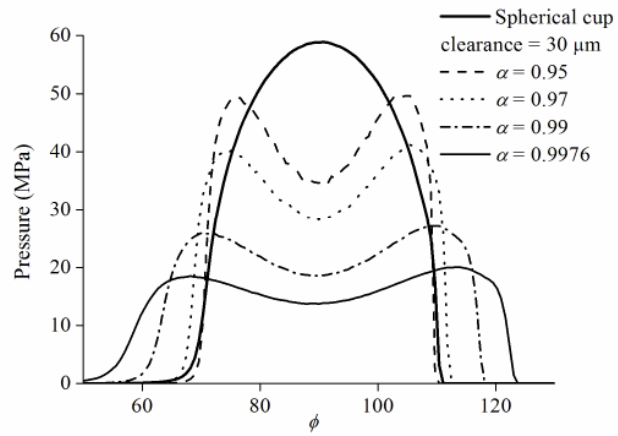
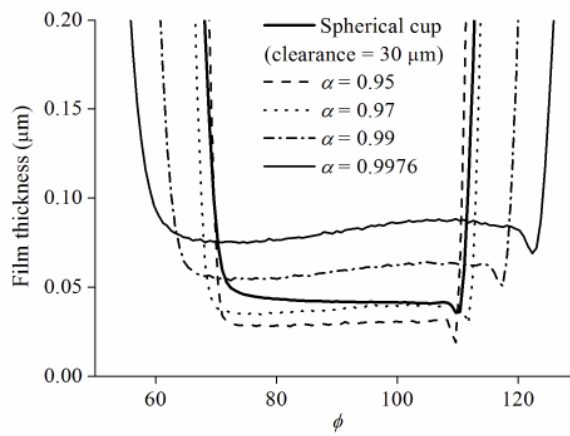


Figure 8



(a)



(b)

Figure 9

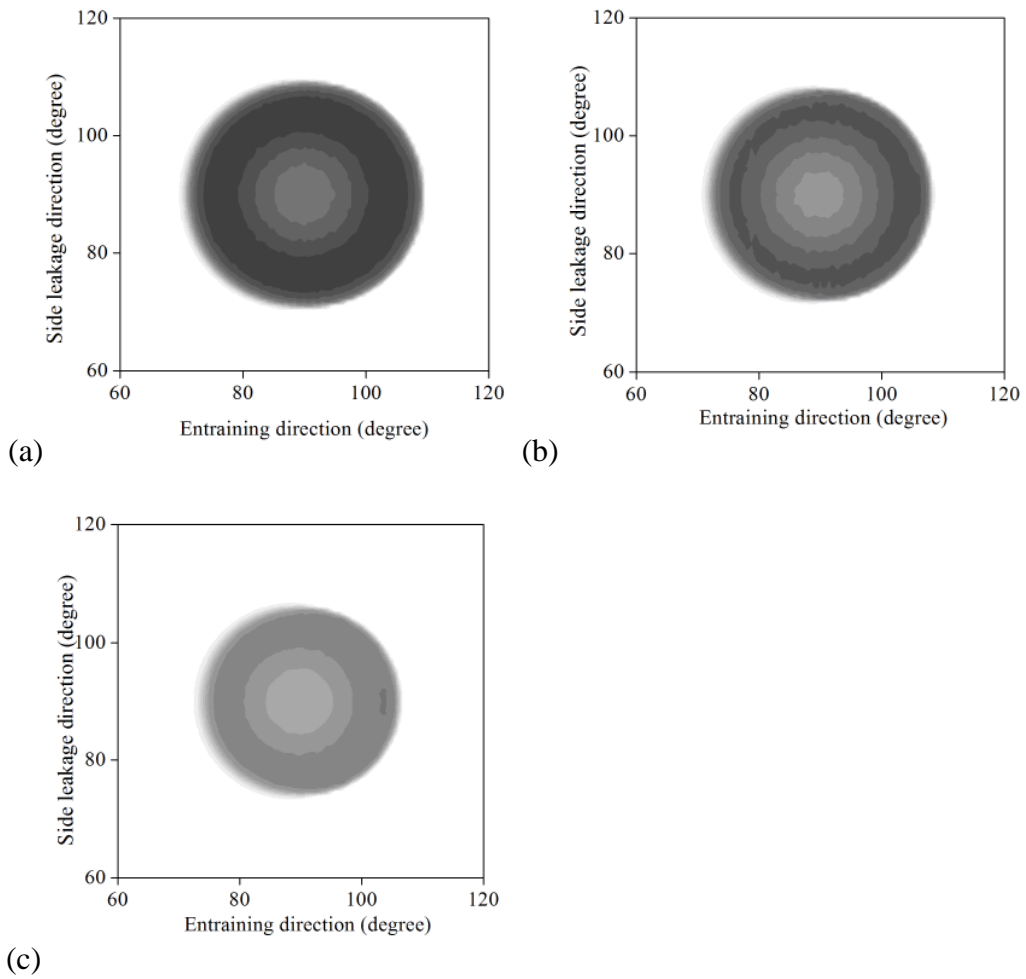
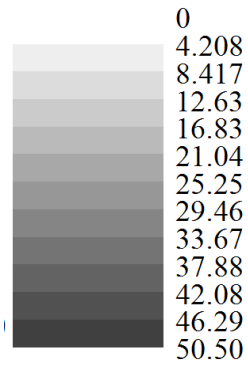
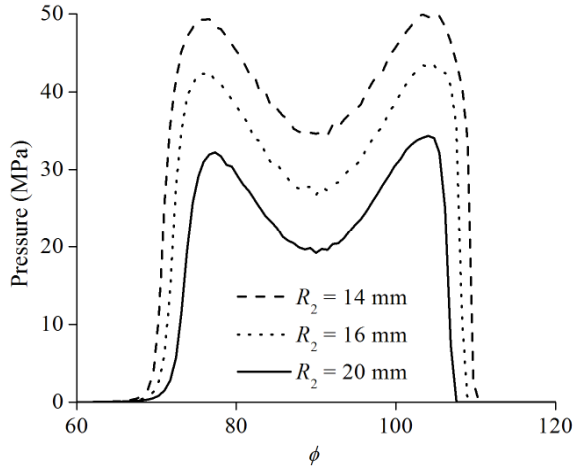


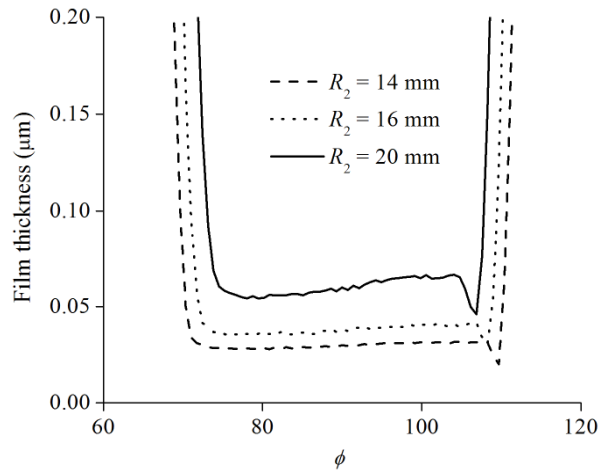
Figure 10

1
2
3
4



(a)

5
6
7
8
9



(b)

10
11
12
13
14
15
16
17
18
19

Figure 11